

# FAST DUAL MINIMIZATION OF WEIGHTED TV + $L^1$ -NORM FOR SALT AND PEPPER NOISE REMOVAL

S. Jehan-Besson

CNRS, UMR 6158, LIMOS, F-63173, Aubière, France

Jonas Koko

Clermont Université, Université Blaise Pascal, LIMOS, BP 10448, F-63000 Clermont-Ferrand, France

CNRS, UMR 6158, LIMOS, F-63173, Aubière, France

**Keywords:** Total variation,  $L^1$  norm, Augmented Lagrangian, Fenchel duality, Uzawa methods, Salt and pepper noise removal.

**Abstract:** In this paper, the minimization of a weighted total variation regularization term (denoted  $TV_g$ ) with  $L^1$  norm as the data fidelity term is addressed using the Uzawa block relaxation method. Numerical experiments show the availability of our algorithm for salt and pepper noise removal and its robustness against the choice of the penalty parameter. This last property is useful to attain the convergence in a reduced number of iterations leading to efficient numerical schemes. The specific role of the function  $g$  in the weighted total variation term is also investigated and we show that an appropriate choice leads to a significant improvement of the final denoising results. Using this function, we propose a whole algorithm for salt and pepper noise removal (UBR-EDGE) that is able to handle high noise levels at a low computational cost.

## 1 INTRODUCTION

In many image processing problems, a denoising step is required to remove noise or spurious details from corrupted pictures. Variational approaches have gained a wide popularity these years due to the possible addition of well-chosen regularity terms. Among the most influential models, we can cite the total variation minimization framework introduced by Rudin and Osher (Rudin and Osher, 1994) and Rudin, Osher and Fatemi (Rudin et al., 1992). In this framework, given a noisy image  $f(x)$ , they propose to recover the original image  $u(x)$  by minimizing the total variation under  $L^2$  data fidelity:

$$E(u) = \int_{\Omega} |\nabla u(x)| dx + \lambda \int_{\Omega} (u(x) - f(x))^2 dx, \quad (1.1)$$

where  $\Omega \subset \mathcal{R}^2$ , is the image domain and  $\lambda$  a positive scale parameter.

Such a minimization allows the recovery of a simple geometric description of the image  $u$  while preserving boundaries. This framework is then very efficient when denoising images with flat zones but fails in preserving texture details. It also fails in removing contrasted and isolated pixels in images corrupted by a salt and pepper noise. For such images, the  $L^1$  norm

is better adapted due to its link to median filtering. It has been used by (Alliney, 1997) and by (Nikolova, 2004; Fu et al., 2006; Bar et al., 2005; Chan et al., 2004; Chan et al., 2005; Cai et al., 2008; Cai et al., 2009) for efficient image denoising algorithms.

In this paper, we choose to investigate the relevance of the  $L^1$  norm for salt and pepper noise removal through the minimization of the following functional where the regularization term is a weighted total variation:

$$E(u) = \int_{\Omega} g(x) |\nabla u(x)| dx + \lambda \int_{\Omega} |u(x) - f(x)| dx, \quad (1.2)$$

where  $g : \Omega \rightarrow \mathcal{R}^+$  is a function independent of  $u$ . Such a criterion has been first investigated in (Bresson et al., 2007) for shape denoising. The function  $g$  was chosen as an edge indicator function of the input image (e.g.,  $g(x) = 1/(1 + |\nabla f|)$ ), which allows a better preservation of corners and sharp angles for shape denoising in images corrupted by a Gaussian noise. In order to use such a criterion for salt and pepper noise removal, we have to consider two main issues: the minimization scheme and the choice of an appropriate function  $g$ .

Concerning the first issue, let us remind that the minimization of the functional (1.2) is not trivial due

its non differentiability. Recent papers addressed the minimization of  $TV + L^1$  using various numerical algorithms. For example, standard calculus of variations and Euler-Lagrange equations can be used to compute the PDE that will drive the functional  $u$  towards a minimum (Bar et al., 2005; Nikolova et al., 2006; Bresson et al., 2007). This method requires a smooth approximation of the  $L^1$  norm and a small time step much be chosen so as to ensure the convergence. This often leads to a large number of iterations as mentioned by (Bresson et al., 2007). In (Chambolle, 2005), the MRF (Markov Random Field) model is based on the anisotropic separable approximation (i.e.  $|\nabla u| = |D_x u| + |D_y u|$  where  $D_x$  and  $D_y$  are the horizontal and vertical discrete derivative operators). This approximation is also used in (Darbon and Sigelle, 2006a; Darbon and Sigelle, 2006b) where the authors proposed an efficient graph-cut method. In all the approaches mentioned above, an approximation or a smoothing of the  $L^1$  norm is required. Recently, in (Bresson et al., 2007), following the works of (Chan et al., 1999; Chambolle, 2004; Aujol and Chambolle, 2005) and more particularly (Aujol et al., 2006), an elegant fast minimization algorithm based on a dual formulation is proposed. Thanks to such approaches, they do not need any approximation or smoothing of the  $L^1$  norm, they rather take benefit of a convex regularization of the criterion which was first proposed by (Aujol et al., 2006).

Following this very interesting work, we propose a new numerical scheme for the minimization of (1.2) using dual methods. From the criterion (1.2), an augmented Lagrangian formulation (Fortin and Glowinski, 1983) with a penalty term is introduced and solved using the block relaxation method of Uzawa. Our algorithm (named UBR) presents the advantage to be more robust to the choice of the penalty parameter than the algorithm proposed by (Bresson et al., 2007). This parameter can then be chosen so as to decrease the number of iterations and consequently the computational cost.

The second contribution of this paper lies in the proposition of a novel algorithm for salt and pepper noise removal. Taking benefit of the weighted total variation term  $TV_g$ , we propose to study the influence of well-chosen functions  $g$  in order to improve the denoising results. An efficient algorithm, denoted UBR-EDGE, is finally proposed for salt and pepper noise removal. Thanks to the nice properties of UBR applied to the weighted TV, our algorithm is able to handle high noise levels at a low computational cost. Experimental results are provided to attest the availability of our 3-steps algorithm.

The paper is organized as follows. In Section

2, we present the  $TV_g + L^1$  model and the Uzawa block relaxation method. The role of the weighted TV for salt and pepper removal and the algorithm UBR-EDGE are presented in section 3 and illustrated with some experimental results.

## 2 EFFICIENT MINIMIZATION OF $TV_g + L^1$ -NORM

Let  $\Omega$  be a two-dimensional bounded open domain of  $\mathcal{R}^d$  with Lipschitz boundary. We consider the following convex energy functional defined, for any  $f \in L^1(\Omega)$ , any  $g : \Omega \rightarrow \mathcal{R}^+$  and any positive parameter  $\lambda$ :

$$E(u) = \int_{\Omega} g(x) |\nabla u(x)| dx + \lambda \int_{\Omega} |u(x) - f(x)| dx \quad (2.1)$$

Our aim is the minimization of the energy functional  $E$ , i.e.

$$\min_{u \in BV(\Omega)} E(u), \quad (2.2)$$

where  $BV(\Omega)$  is the subspace of functions  $u \in L^1(\Omega)$  of bounded variations.

### 2.1 An Augmented Lagrangian Method

In order to approximate (2.1) by an augmented Lagrangian and to present our dual method of resolution, we need to transform the convex minimization problem into a suitable saddle-point problem by introducing an auxiliary unknown. Let us introduce the auxiliary unknown  $p = f - u$  and rewrite the functional  $E$  as

$$E(u, p) = \int_{\Omega} g(x) |\nabla u(x)| dx + \lambda \int_{\Omega} |p(x)| dx \quad (2.3)$$

The unconstrained minimization problem becomes

$$\min_{(u,p) \in K} E(u, p). \quad (2.4)$$

where  $K = \{(u, p) \in X \times X \mid u + p - f = 0 \text{ in } X\}$ , with the Euclidian space  $X = \mathcal{R}^{N \times N}$  equipped with the  $L^2$  scalar product  $(u, v)$ . To problem (2.4), we associate the augmented Lagrangian functional (see (Koko and Jehan-Besson, 2009) for details) defined by:

$$\begin{aligned} \mathcal{L}_r(u, p; s) &= E(u, p) + (s, u + p - f) \\ &+ \frac{r}{2} \|u + p - f\|^2, \end{aligned} \quad (2.5)$$

where  $r > 0$  is the penalty parameter and  $s$  the Lagrange multiplier. This minimization problem can be solved using Uzawa block relaxation methods which

have been used in nonlinear mechanics for operator splitting and domain decomposition methods (Fortin and Glowinski, 1983; Glowinski and Tallec, 1989; Koko, 2008). Applying the block relaxation method to the problem defined above, we obtain the following algorithm:

### Minimization process of $TV_g + L^1$

**Initialization.**  $p^{-1}$ ,  $s^0$  and  $r > 0$  given.

$k \geq 0$ . Compute successively  $u^k$ ,  $p^k$  and  $s^k$  as follows.

**Step 1.** Find  $u^k \in X$  such that

$$\mathcal{L}_r(u^k, p^{k-1}; s^k) \leq \mathcal{L}_r(v, p^{k-1}; s^k), \quad \forall v \in X. \quad (2.6)$$

**Step 2.** Find  $p^k \in X$  such that

$$\mathcal{L}_r(u^k, p^k; s^k) \leq \mathcal{L}_r(u^k, q; s^k), \quad \forall q \in X. \quad (2.7)$$

**Step 3.** Update the Lagrange multiplier

$$s^{k+1} = s^k + r(u^k + p^k - f).$$

The algorithm UBR corresponds to the generic block relaxation algorithm ALG2 (see, e.g., (Fortin and Glowinski, 1983; Glowinski and Tallec, 1989)). Let us now detail the explicit solutions of the different steps (proofs are given in (Koko and Jehan-Besson, 2009)).

**Proposition 2.1** *The solution of Step 1 can be given by:*

$$u^k = f - p^{k-1} + \frac{1}{r}(\nabla \cdot v^* - s^k)$$

where  $v^*$  is the solution of:

$$-\nabla(\nabla \cdot v^* - \tilde{p}^{k-1}) + \frac{1}{g}|\nabla(\nabla \cdot v^* - \tilde{p}^{k-1})|v^* = 0. \quad (2.8)$$

with  $\tilde{p}^{k-1} = s^k + r(p^{k-1} - f)$ .

For solving (2.8), we can use the fixed-point procedure of Chambolle (Chambolle, 2004),  $v^0 = 0$  and for any  $\ell \geq 0$

$$v^{\ell+1} = \frac{v^\ell + \tau \nabla(\nabla \cdot v^\ell - \tilde{p}^{k-1})}{1 + (\tau/g)|\nabla(\nabla \cdot v^\ell - \tilde{p}^{k-1})|}, \quad (2.9)$$

where  $\tau > 0$ .

The solution of Step 2 is detailed in (Koko and Jehan-Besson, 2009) and reminded below in the whole description of the algorithm:

### Algorithm UBR

**Initialization.**  $p^{-1}$ ,  $s^0$  and  $r > 0$  given.

**Iteration**  $k \geq 0$ . Compute successively  $u^k$ ,  $p^k$  and  $s^k$  as follows.

**Step 1.** Set  $\tilde{p}^{k-1} = s^k + r(p^{k-1} - f)$  and compute  $v^k$  with (2.9).

Compute  $u^k$

$$u^k = f - p^{k-1} + \frac{1}{r}(\nabla \cdot v^k - s^k)$$

**Step 2.** Compute  $p^k$

$$p^k = \begin{cases} 0 & \text{if } |s^k + r(u^k - f)| < \lambda, \\ f - u^k - \frac{1}{r} \left[ s^k - \lambda \frac{s^k + r(u^k - f)}{|s^k + r(u^k - f)|} \right] & \text{if } |s^k + r(u^k - f)| \geq \lambda. \end{cases}$$

**Step 3.** Update the Lagrange multiplier

$$s^{k+1} = s^k + r(u^k + p^k - f).$$

We iterate until the relative error in  $u^k$  and  $p^k$  becomes sufficiently “small”. The convergence of the algorithm UBR is checked using the following convergence criterion:

$$\frac{\sqrt{\|u^k - u^{k-1}\|_2^2 + \|p^k - p^{k-1}\|_2^2}}{\sqrt{\|u^k\|_2^2 + \|p^k\|_2^2}} \leq \varepsilon_{up}.$$

The discrete divergence and gradient operators are given in (Chambolle, 2004).

Note that, each iteration of Algorithm UBR requires the convergence of the Chambolle fixed point procedure (2.9). The convergence of this loop is checked using a threshold on the normalized  $L^2$  error on  $v^\ell$ .

## 2.2 Applicability and Robustness

We first test the availability of our UBR algorithm for salt and pepper noise removal taking classically  $g = 1$  which corresponds to the minimization of  $TV + L^1$ . The experimental results provided in Figure 1 demonstrate that noise is correctly removed. Moreover, the noisy part is captured through the auxiliary unknown  $v$  as displayed in Figure 1.c. With the function  $g(x) = 1$  and  $\lambda = 1.5$ , we find a PSNR of 32.5 dB for the denoising of a noise of 10%. The parameter  $\lambda$  is a classical smoothing parameter. Choosing a smaller value leads to a higher blurring of image components. The influence of this parameter is less sensitive when using the  $TV_g$  regularization term as demonstrated in the next section.

In a second step, we want to study the robustness of the result against the choice of the parameter  $r$ . Our experimental results tend to prove that the algorithm UBR provides the same denoised images for different values of  $r$ . This is demonstrated by the Figure 2 that displays the evolution of the PSNR according to the number of iterations for different parameters  $r$  (from



(a) Noisy image

(b) Final  $u$ (c) Final  $v$ 

Figure 1: The images  $u$  (PSNR= 32.5dB) and  $v$  obtained after convergence of the algorithm UBR with  $g(x) = 1$  ( $\lambda = 1.5$ ,  $r = 20$ ,  $\epsilon_{up} = 0.0001$ ) for the image “peppers” with a salt and pepper noise of 10%.

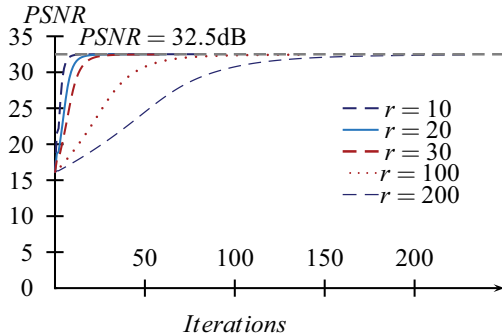


Figure 2: Algorithm UBR ( $g=1$ ) : Evolution of PSNR during iterations ( $\lambda = 1.5$ ) with  $r = 10, 20, 30, 100, 200$  ( $\epsilon_{up} = 0.0001$ ) for the image “peppers” with a salt and pepper noise of 10%.

10 to 200). Such a feature then represents an improvement of the method proposed in (Bresson et al., 2007) since the convergence can be obtained without the need to increase  $r$  to infinity. We also report the number of iterations according to  $r$  (Figure 3). In this case, the optimal value in terms of iterations is obtained for  $r = 30$  with 60 iterations when  $\lambda = 1.5$ , and for  $r = 10$  with 91 iterations when  $\lambda = 0.5$ . Choosing a higher value for  $r$  increases the number of iterations needed to attain the convergence without improving the final result. We can then choose a small value for  $r$  to obtain a low computational cost without decreasing the quality of the result.

### 3 SALT AND PEPPER NOISE REMOVAL

In this section, we first propose to take benefit of the weighted TV regularization term and of a dedicated function  $g$  in order to increase the quality of the denoising results. Our algorithm UBR is then embedded in a more complete process specified for salt and pepper noise removal and named UBR-EDGE.

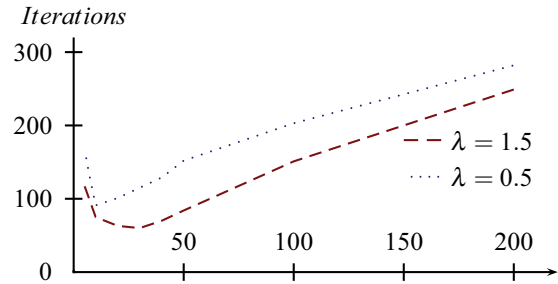


Figure 3: Algorithm UBR ( $g=1$ ) : Number of iterations for convergence according to the parameter  $r$  with  $\lambda = 0.5$  and  $\lambda = 1.5$  for the image “Peppers” with a salt and pepper noise of 10%.

#### 3.1 The Role of the Weighted TV

A first improvement of the denoising results can be obtained using the fact that the dynamic range of the noise is known. Indeed corrupted pixels take the values  $min$  or  $max$  that correspond respectively to the minimum and maximum values of intensity. In order to embed this information in the function  $g$ , we introduce the following mask function:

$$m(x) = \begin{cases} \alpha_n & \text{if } f(x) = \min \text{ or } \max \\ \alpha & \text{elsewhere.} \end{cases} \quad (3.1)$$

We choose  $\alpha_n = 1.5$  and  $\alpha = 0.5$  in order to up-permost smooth the corrupted pixels. We then take  $g(x) = m_\sigma(x)$  where  $m_\sigma(x) = G_\sigma * m(x)$  is a slight regularized version of  $m$  ( $G$  is a Gaussian of 0-mean and variance  $\sigma = 0.5$ ).

Figure 4 displays the resulting images and the corresponding values of PSNR while setting  $g(x) = 1$  (first row) and  $g(x) = m_\sigma(x)$  (second row). Final images are provided for different values of the regularization parameter  $\lambda$ . For each parameter, we observe a significant increase of 2 to 4dB in the final PSNR. The best value of PSNR is 34.9 dB obtained for  $\lambda = 1.5$ . The scale effect of the parameter  $\lambda$  is also less visible due to the fact that we restrict the regularization term to the extreme values of intensities corresponding to the corrupted pixels.

Moreover, these first results are obtained at a low computational cost (from 1.6 seconds for a noise of 10% to 4.3 seconds for a noise of 70% on the image Peppers (256x256) with a computer of 3GHz and 2Gb of RAM). This confirms the efficiency of our numerical scheme UBR and attests its availability for the design of our 3-steps salt and pepper noise removal algorithm detailed thereafter.

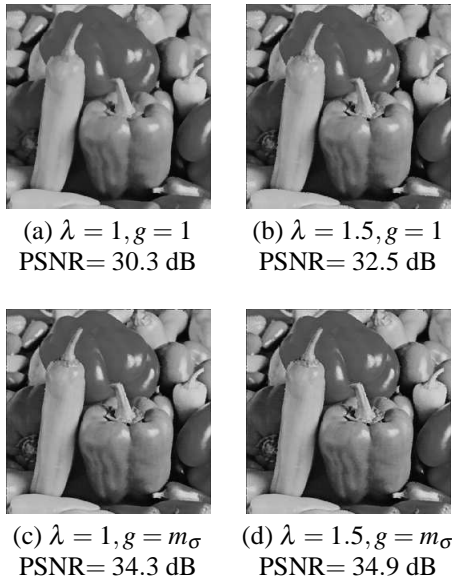


Figure 4: Experimental results with the algorithm UBR for different smoothing values of  $\lambda$  ( $r = 20, \varepsilon_{up} = 0.0001$ ) for the image “peppers” with a salt and pepper noise of 10%. The first row displays the results obtained with  $g(x) = 1$  while the second row displays the result obtained using  $g(x) = m_\sigma(x)$ .

### 3.2 The 3-steps Algorithm UBR-EDGE

The use of the weighted TV provides a significant increase of the quality of the final results. However, even if the algorithm  $TV_g + L^1$  well performs for low noise values, it gives very smoothed results for higher noise values. Indeed, in order to remove large noisy patches, we must decrease the parameter  $\lambda$  and so increase the smoothing of the whole image. In order to circumvent such a problem, we propose both a pre and post-processing to UBR. As a first step (pre-processing), we propose to decrease the size of unknown values (corrupted pixels) using a median filter (of half-size 1). The pixels that are still corrupted after this first pass are estimated by computing a mean on the known 4-connexity neighbours (i.e. we only take the known values to compute the mean). The aim of this first pass is to correct the bias introduced by the extreme intensity values of the noisy pixels (*min* or *max*) in the variational process. This first estimation is then corrected using the  $TV_g + L^1$  algorithm which is able to smooth differently noisy pixels from uncorrupted ones through the  $g$  function. This function is chosen to be  $m_\sigma(x)$  detailed in section 3.1. The corrupted pixels are computed from the input image but the function  $f$  used in UBR is the result of step 1. At the end of the process, we apply a very simple edge smoother also known as EDDI (De Haan and Lodder, 2002) usually used in de-interlacing process for

electronic devices. In this efficient edge smoother, the unknown intensity values are estimated by computing the mean between the two opposite pixels that share the nearest intensity in a 8-neighborhood. We apply this simple filtering scheme only on the initial corrupted pixels.

#### Algorithm UBR-EDGE

##### Step 1. Pre-processing

$f_1 \leftarrow \text{median-filter}(f, 1)$   
 if  $f_1(x) = \min$  or  $f_1(x) = \max$  then

$$f_1(x) = \frac{1}{\sum_{x_i \in V_4(x)} w(f(x_i))} \sum_{x_i \in V_4(x)} w(f(x_i))f(x_i)$$

with  $w(f(x_i)) = 0$  if  $f(x_i) = \min$  or  $\max$ .

##### Step 2. Algorithm UBR

run UBR with  $f_1$  as the input image and  $g(x) = m_\sigma(x)$  defined in (3.1) and computed using the initial image  $f$ .

##### Step 3. Edge smoother

if  $f(x) = \min$  or  $f(x) = \max$  then

$$u = 0.5 * (u(x_i + l, x_j + k) + u(x_i - l, x_j - k))$$

where

$$(l, k) = \underset{(l, k) \in \{-1, 1\} \times \{-1, 1\}}{\operatorname{argmin}} \operatorname{diff}(l, k)$$

with  $\operatorname{diff}(l, k) = |u(x_i + l, x_j + k) - u(x_i - l, x_j - k)|$ .

Let us remark that the first functional  $f_1$  only acts as an initial condition of the algorithm UBR in order to give a first rough estimate for the corrupted pixels. The last edge smoother is applied only on the corrupted pixels as well.

In Figure 5, final results of the different steps of our process are given for the restoration of the image “Lena” corrupted by a salt and pepper noise of 70%. The Figure 5.(b) displays the image obtained after the pre-processing step (median filter + mean). This image is processed as an input of our algorithm UBR using  $g(x) = m_\sigma(x)$  and the result of our UBR algorithm is given in Figure 5.(c). The EDGE smoother EDDI is then applied which gives the final image of Figure 5.(d).

### 3.3 Experimental Results

Some visual results are provided in Figure 6 for “Lena” (512x512) and in Figure 7 for “Peppers” (256x256). Thanks to these visual results and to the associated PSNR values and computational costs reported for all the noise levels in Table 8, we can conclude that our algorithm provides good visual results

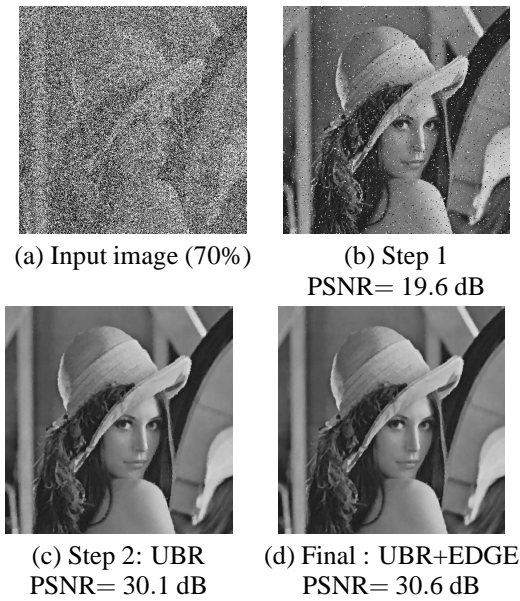


Figure 5: Salt and pepper noise removal using the algorithm UBR-EDGE for the image Lena corrupted by a noise of 70%. The result is given for each step of the process. The image obtained after the pre-processing (median+mean) is given in (b). This image is used as an input of the algorithm UBR and the result is given in (c). A last post-processing is applied to the image which yields to the final result given in (d).

at a low computational cost. The PSNR values obtained for the image “Lena” can be compared with the PSNR values reported in (Chan et al., 2004; Chan et al., 2005) for many different algorithms. Compared to the values computed in this paper, our algorithm gives comparable PSNR results to the best algorithm (i.e. algorithm III) even for a high noise level. For completeness, we report the values given by (Chan et al., 2005) for the denoising of Lena (512x512) with a noise of 70%. With the classical Median filter, the PSNR is 23.2dB and with an improved switching median (ISM) filter, the PSNR is 23.4dB. Using the algorithm III proposed in (Chan et al., 2005), the PSNR is 29.3dB. We find a PSNR of 31.4 dB using our algorithm. For a noise of 90%, they find a PSNR of 25.4 dB while our algorithm gives a PSNR of 26.6 dB. We also run our algorithm on the input noisy images provided in the web page of R. Chan <sup>1</sup>. Experimental results reported in (Koko and Jehan-Besson, 2009) show that our algorithm gives good quality results with a PSNR value that is a little smaller than the one found by the algorithm III (Chan et al., 2004)(with a difference of less than 1 dB). More precisely, for the denoising of the first image in Figure 6.a (noise of 70%), they find a PSNR of 23.07dB while our

<sup>1</sup><http://www.math.cuhk.edu.hk/~rchan/paper/impulse/>

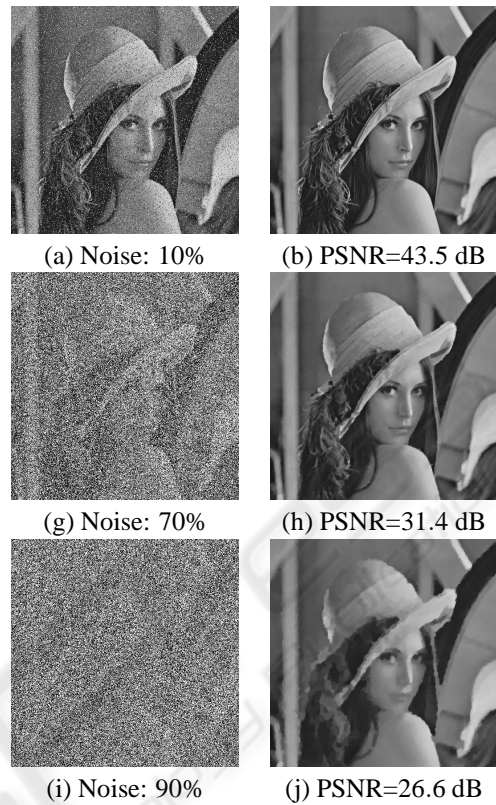


Figure 6: Salt and pepper noise removal using the algorithm UBR-EDGE for the image Lena (512x512). The input images are given with the associated results.

PSNR is 22.2dB. For the image 6.b, they find a PSNR of 34.16dB while our is 33.3dB. For the image 6.c, they find a PSNR of 26.78dB while our is 26.0dB. So their algorithm gives better PSNR for these images but with a difference of less than 1dB. As far as the computational cost is concerned, it is difficult to compare the two computational costs since the algorithm III is programmed using Matlab. However, our algorithm seems to provide a lower computational cost especially for a high level of noise (see Table 8).

## 4 CONCLUSIONS

In this paper, our contribution is twofold. First, we propose a new efficient and robust minimization scheme for the minimization of a  $TV_g + L^1$  criterion using Uzawa Block Relaxation (UBR) method. We more particularly study the robustness of the algorithm against the penalty parameter  $r$ . Secondly, we investigate the role of the weighted TV to improve salt and pepper noise removal and we embed our algorithm in an efficient 3-steps process dedicated to high noise levels. Our algorithm gives comparable

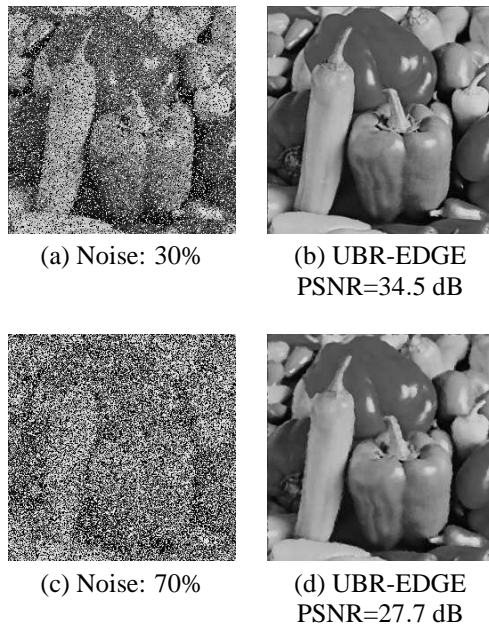


Figure 7: Salt and pepper noise removal using the algorithm UBR-EDGE for “Peppers”. For the result obtained in (b),  $\lambda=2$  and for the result in (d),  $\lambda = 1.5$ .

Noise	Algorithm UBR-EDGE			
	Lena (512x512)		Peppers (256x256)	
	PSNR	time(s)	PSNR	time(s)
10	43.4	2.7	40.6	0.4
20	39.7	3.9	37.3	0.7
30	37.1	5.3	34.5	1.1
40	35.3	6.6	32.2	1.4
50	33.9	8.1	30.6	1.7
70	31.4	17.1	27.7	2.3
90	26.6	41.4	23.1	20.1

Figure 8: PSNR according to the salt and pepper noise level for the image “Peppers” (256x256) and “Lena” (512x512) using the algorithm UBR-EDGE ( $r = 200$ ,  $\epsilon_{up} = 0.0001$ ). For a noise level between 10% and 50%, we choose the same value of  $\lambda = 2$ . For a noise level of 70%,  $\lambda = 1.5$  and for 90%,  $\lambda = 0.7$ .

PSNR values to one of the best denoising algorithm available in the literature and at a lower computational cost. However, we can mention that choosing automatically the value of both the scale parameter and the penalty parameter in order to obtain the best quality result and the lower computational cost is an open question that remains difficult to solve. Our on going research is directed towards this issue.

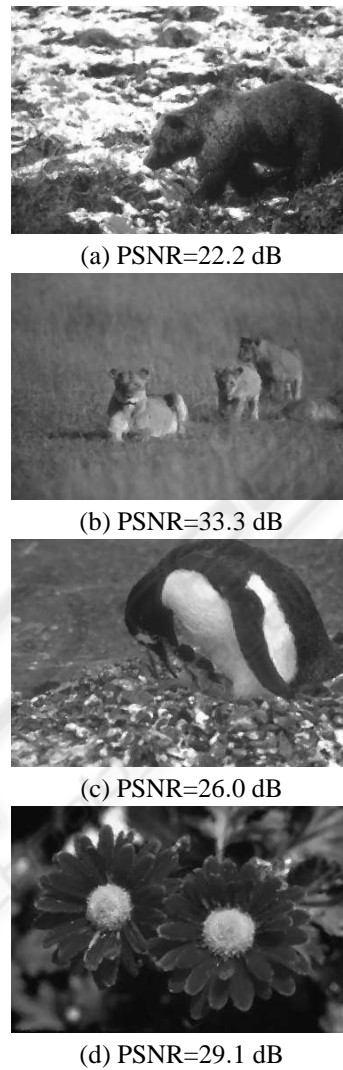


Figure 9: Salt and pepper noise removal using the algorithm UBR-EDGE for different images of the Berkeley database corrupted with a salt and pepper noise of 70%. For all the results, we take  $\lambda = 2$ .

## ACKNOWLEDGEMENTS

The numerical experiments were run in C++ with the library Pandore<sup>2</sup>. The salt and pepper noise was generated with gmic<sup>3</sup>.

## REFERENCES

Alliney, S. (1997). A property of the minimum vectors of a regularizing functional defined by means of the abso-

<sup>2</sup>available at <http://www.greyc.ensicaen.fr/regis/Pandore/>

<sup>3</sup><http://gmic.sourceforge.net/>

- lute norm. *IEEE Transactions on Signal Processing*, 45(4):913–917.
- Aujol, J.-F. and Chambolle, A. (2005). Dual norms and image decomposition models. *International Journal of Computer Vision*, 63(1):85–104.
- Aujol, J.-F., Gilboa, G., Chan, T. F., and Osher, S. (2006). Structure-texture image decomposition - modeling, algorithms, and parameter selection. *International Journal of Computer Vision*, 67(1):111–136.
- Bar, L., Sochen, N. A., and Kiryati, N. (2005). Image deblurring in the presence of salt-and-pepper noise. In Kimmel, R., Sochen, N. A., and Weickert, J., editors, *Scale-Space*, volume 3459 of *Lecture Notes in Computer Science*, pages 107–118. Springer.
- Bresson, X., Esedoglu, S., Vandergheynst, P., Thiran, J.-P., and Osher, S. (2007). Fast global minimization of the active contour/snake model. *Journal of Mathematical Imaging and Vision*, 28:151–167.
- Cai, J., Chan, R., and Nikolova, M. (2008). Two-phase methods for deblurring images corrupted by impulse plus gaussian noise. *Inverse Probl. Imaging*, 2:187–204.
- Cai, J., Chan, R., and Nikolova, M. (2009). Fast two-phase image deblurring under impulse noise. *Journal of Mathematical Imaging and Vision*.
- Chambolle, A. (2004). An algorithm for total variation minimization and applications. *Journal of Mathematical Imaging and Vision*, 20(1-2):89–97.
- Chambolle, A. (2005). Total variation minimization and a class of binary MRF models. In *Workshop on Energy Minimization Methods in Computer Vision and Pattern Recognition*, pages 136–152.
- Chan, R., Ho, C., and M. Nikolova (2005). Salt-and-pepper noise removal by median-type noise detectors and detail-preserving regularization. *IEEE Transactions on Image Processing*, 14(15):1479–1485.
- Chan, R., Hu, C., and Nikolova, M. (2004). An iterative procedure for removing random-valued impulse noise. *IEEE Signal Processing Letters*, pages 921–924.
- Chan, T., Golub, G., and P. Mulet (1999). A nonlinear primal-dual method for total variation-based image restoration. *SIAM Journal of Scientific Computing*, 20(6):1964–1977.
- Darbon, J. and Sigelle, M. (2006a). Image restoration with discrete constrained total variation part I: Fast and exact optimization. *Journal of Mathematical Imaging and Vision*, 26(3):261–271.
- Darbon, J. and Sigelle, M. (2006b). Image restoration with discrete constrained total variation part II: Levelable functions, convex priors and non convex cases. *Journal of Mathematical Imaging and Vision*, 26(3):277–291.
- De Haan, G. and Lodder, R. (2002). De-interlacing of video data using motion vectors and edge information. In *International Conference on Consumer Electronics*, pages 70–71.
- Fortin, M. and Glowinski, R. (1983). *Augmented Lagrangian Methods: Application to the Numerical Solution of Boundary-Value Problems*. North-Holland, Amsterdam.
- Fu, H., Ng, M. K., Nikolova, M., and Barlow, J. L. (2006). Efficient minimization methods of mixed l2-l1 and l1-l1 norms for image restoration. *SIAM J. Scientific Computing*, 27(6):1881–1902.
- Glowinski, R. and Tallec, P. L. (1989). *Augmented Lagrangian and Operator-splitting Methods in Nonlinear Mechanics*. SIAM, Philadelphia.
- Koko, J. (2008). Uzawa block relaxation domain decomposition method for the two-body contact problem with Tresca friction. *Comput. Methods. Appl. Mech. Engrg.*, 198:420–431.
- Koko, J. and Jehan-Besson, S. (2009). An augmented lagrangian method for TVg+L1-norm minimization. *Technical Report RR-09-07, Laboratory LIMOS*.
- Nikolova, M. (2004). A variational approach to remove outliers and impulse noise. *Journal of Mathematical Imaging and Vision*, 20(1-2):99–120.
- Nikolova, M., Esedoglu, S., and Chan, T. F. (2006). Algorithms for finding global minimizers of image segmentation and denoising models. *SIAM Journal of Applied Mathematics*, 66(5):1632–1648.
- Rudin, L. and Osher, S. (1994). Total variation based image restoration with free local constraints. In *ICIP*, volume 1, pages 31–35, Austin, Texas.
- Rudin, L., Osher, S., and Fatemi, E. (1992). Nonlinear total variation based noise removal algorithms. *Physica D.*, 60:259–268.